

PANAMA

PRESCRIPTIVE SOLAR ANALYTICS & ADVANCED WORKFORCE MANAGEMENT

D2.1

„Software modules from T2.1, T2.2, T2.3”

Responsible Partner	AIT
Prepared by	Bernhard Kubicek
Checked by WP Leader	

Planned Submission Date	31.10.2020
Actual Submission Date	31.11.2021
Status and Version	Final



Project PANAMA is supported under the umbrella of SOLAR-ERA.NET Cofound by the Austrian Research Promotion Agency (FFG), General Secretariat for Research and Technology (GSRT) and the Scientific and Technological Research Council of Turkey (TUBITAK).

Table of Contents

EXECUTIVE SUMMARY	3
1. Results of Milestone 2.1	4
1.1 Inverter Analytics	4
1.2 MPP Analytics:.....	6
2. Results of Milestone 2.2	9
2.1 Digital Twins	9
2.1.1 Timestamp validation and orientation estimation.....	11
2.1.2 Data reduction for model fitting	13
2.1.3 Evaluation of the digital twin	13
2.2 PID.....	14
2.3 Soiling.....	15
3. Results of Milestone 2.3	16
3.1 Digital Twins	16
3.1.1 Preprocessing.....	18
3.1.2 Twin Modeling	18
3.1.3 AI assisted twinning	21
3.1.4 Prediction of power likelihood	22
3.1.5 Total prediction digital twin + Uncertainty	23
3.2 Extrapolation to plants with no history.....	24
3.3 Revenue Loss.....	24
3.4 System Integration.....	24

EXECUTIVE SUMMARY

Within the PANAMA project, the milestone 2.3 is the outcome of the Task 2.3. Both are due at the 14th project month, which is the end of August 2021.

Within Task 2.1, failure diagnosis routines were developed that detect and classify system failures by analyzing acquired system data. More specifically, the main exhibited failures on PV modules and inverters are profiled in order to build models that compare data feeds and detect abnormal performance operating conditions. Detected abnormal operating conditions (obtained by comparing data feeds against set threshold levels and modelled expected performance) are then passed to the final classification stage. The routines perform real-time comparisons against the known failure profiles in order to first identify and then quantify the loss. Human experts typically perform visual inspection of monitoring data using graphs and plots. With the developed methodology, the content of virtual plots is evaluated automatically, to extract metrics that describe features relevant to failure mechanisms. E.g. the ratio of low light to strong irradiations typical tracking voltage can be used to exhibit PID.

Furthermore, cyclic changes of these parameters are evaluated, i.e. in daily or seasonal changes, to exhibit even more information about the systems.

Virtual plot analysis is performed for both the inverter efficiency as well as the MPP tracking data cloud, to exhibit both problems of the inverter or the module strings independently.

Within Task 2.2, trend-based performance loss rate (degradation, PID, shading and soiling) algorithms were developed in order to detect and predict underperforming conditions at early stages. In particular, regressive time series analysis techniques (ordinary least squares, classical seasonal decomposition, autoregressive moving average, etc.) were investigated for calculation of the degradation rate of PV systems.

This is done using a historically fitted analytic digital twins, that in an innovative second stage use black box AI to improve the prediction accuracy. Furthermore, the typical deviation of the prediction are also estimated. Comparison between sensor based nowcasting and actual system production allows to detect soiling, shading and of course common degradation.

Results of Task 2.3, the digital twin, were merged with the results of Task 2.2, as the digital twin is actually integral to finding trend based degradation methods.

1. Results of Milestone 2.1

While monitoring larger Photovoltaic (PV) generators (“plants”), typically there are three different sources of data: data recorded by inverters, weather sensors, and finally the electric meters. Most commonly, data is uploaded to a web-based data platform.

From there, data can be downloaded for further analysis. Most commonly, the data is provided in text files.

Typical data from inverters contains on the AC side: power, grid frequency and phase currents. On the module DC side, commonly the working point is recorded (U_mpp, I_mpp) for possibly multiple MPP trackers per inverter.

1.1 Inverter Analytics

By calculating the inverter efficiency from monitoring data, quantitative information can be obtained. Along the two-dimensional efficiency characteristics only a small subsection is traversed during a typical day by the inverter. Therefore, point clouds with the horizontal axis being the irradiation, and the vertical axis being the efficiency can be used for further analysis. These point clouds can additionally be colored by features (module temperature, day hour, day in year, etc.) to analyze possible deviations from normal operation. Furthermore, a 2D histogram reflecting the density of points can be obtained, that makes certain behavior more visible as shown in Figure 1.

In many model designs, large inverters are assemblies of similar sub-blocks (modular design). Under low production conditions, efficiency can be improved by deactivating some of these blocks, operating each active block at its optimum conversion efficiency. The switching conditions require a hysteresis setting in the firmware. A failure of this switching operation, as observed in previous projects, as shown in Figure 1.

From these graphs, scalar metrics can be extracted by defining regions of interest and performing statistical analysis on all data points that are contained therein, see also figures 2 and 3. For larger systems, these values are then reported in data tables.

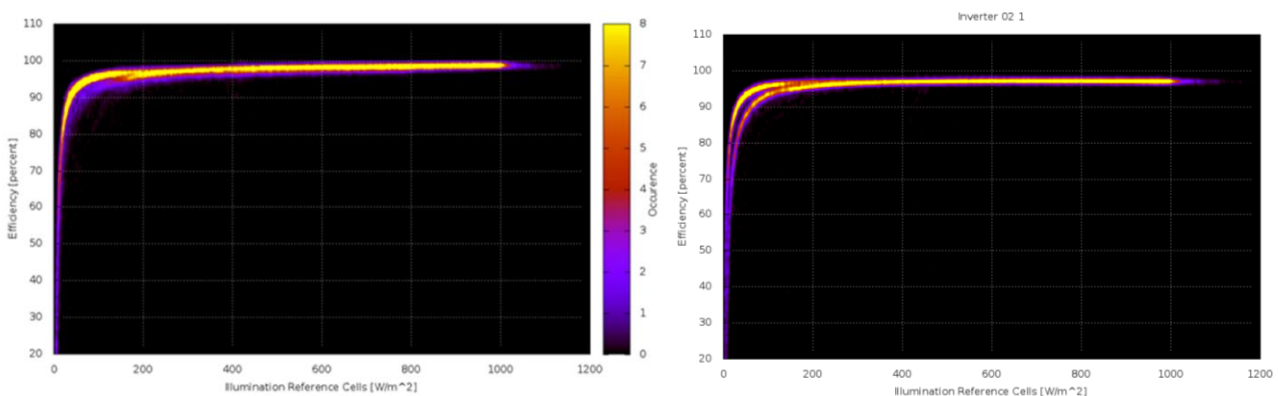


Figure 1: Left, a normal operation of an exemplary inverter. At 150W/m² irradiation, the switching of inverter blocks occurs. Right: Here, clearly the firmware has problems choosing the correct amount of active sub-blocks, creating a bad structure that is distinguishable by the day hour.

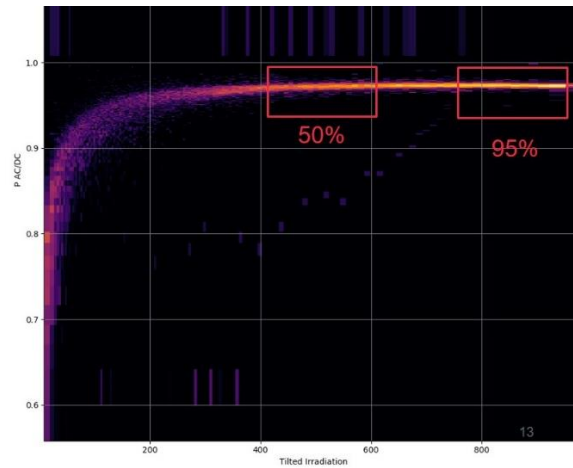


Figure 2 : Two-dimensional histogram of the density of points (irradiation, inverter efficiency). The region of interest that are evaluated to the half and full power efficiency are indicated.

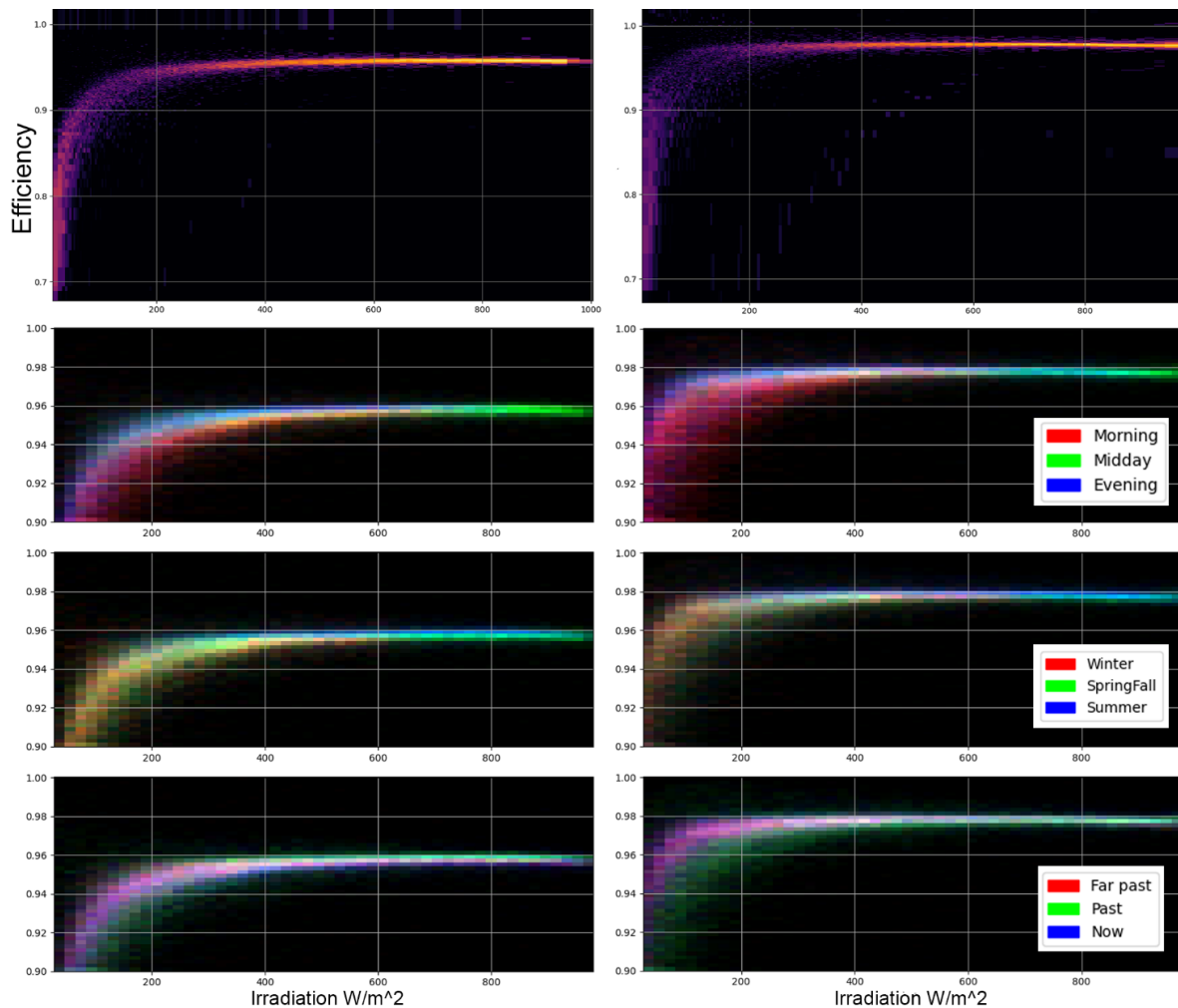


Figure 3: Comparison of exemplary inverters. The 2D histogram point density (top) was additionally colorized with three features using additive color mixing. Hence, an overlap of “red” and “blue” appears “violet”. Using the colorizations, additional structures can be observed: In the right example, in the evening the inverter efficiency is slightly better than in the morning hours. The last row of figures labels the current year in blue, the year before in green, and the second-last year in red, e.g. to exhibit potential inverter degradation.

1.2 MPP Analytics:

In typical inverters, the DC voltage and current are monitored, while an additional sensor monitors irradiation in the module plane as well as the module temperatures. While it is clear, that the module temperature varies between different locations in the PV-plant, and even, depending on the location, on the backside of a single module, it reflects the general trend of temperatures.

A changing irradiation causes the maximum power point (MPP: voltage V/ current I) to change, leading to the well-known IV characteristic of PV cells and modules, see Figure 4 (depending on module type, cable resistance and other losses). The red highlighted shape of the MPP tracking line can also be observed in the corresponding plot of the monitoring data, although less pronounced, see Figure 5. Many of the deviations from the ideal line originate from volatile irradiation conditions, where the inverter is not fast enough to follow the changing MPP.

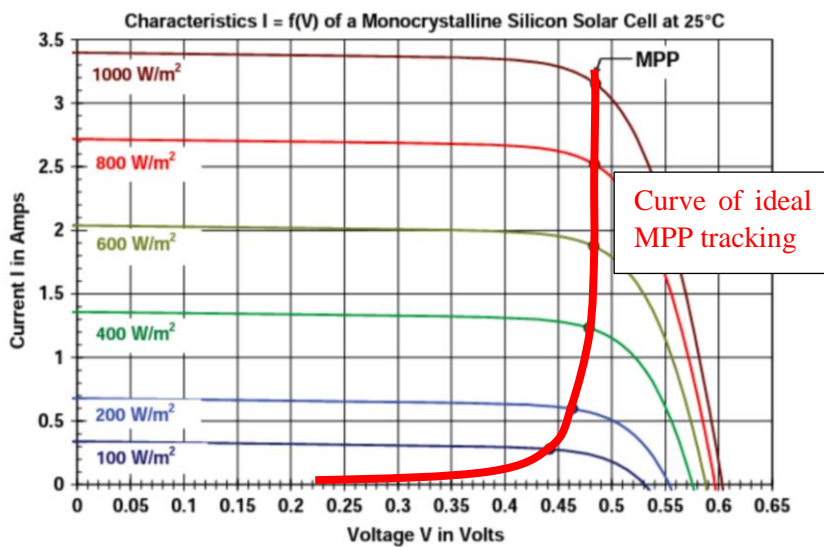


Figure 4: The MPP, apart from a small temperature effect, strongly depends on the irradiation (red curve). For larger irradiations, the voltage stays mostly constant, while the current is proportional to the irradiance. However, for less than 150W/m², the power decreases towards zero, causing a larger than linear decrease of production compared to irradiation.

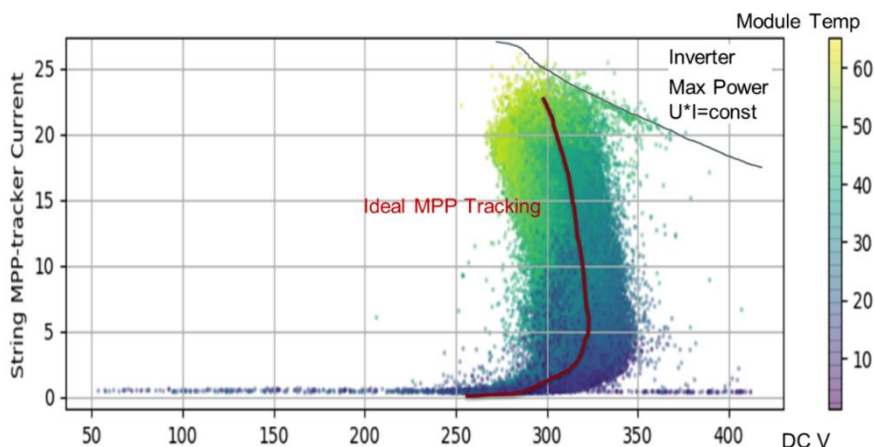


Figure 5: The inverters monitor the MPP voltage and current, and the corresponding point cloud shows quite a diffuse expansion that is typically centered around the theoretical MPP (irradiation) curve.

A small additional variation of the shapes would occur due to the module temperature and its effect on the MPP, which is mostly avoided by using a temperature corrected MPP voltage in the plots. The power at MPP itself has a well-known correction coefficient, that is stated e.g. in data sheets. The temperature coefficient of the open circuit voltage (U_{oc}) is typically ~ 10 times larger than the coefficient of the short circuit current (I_{sc}). This justifies the approximation of only correcting the voltage of the MPP data points using a factor slightly less than the one for U_{oc} .

The MPP-clouds can be colorized with additional features, see Figure 6. Methods suitable for automatic processing can be used to extract metrics from graphs to avoid the manual inspection of a huge amount of graphical information. This is performed using regions of interest, see Figure 7. Furthermore, from a set of data multiple MPP clouds can be created, that are distinguished by feature groups: e.g. hours of the day, months, quarters, or years. From these sets of clouds, again the scalar features can be extracted, and plotted over the index of the feature group. This enables to plot the change of the MPP voltage or current over the time of day, the season, see Figure 8, or in accordance for long-term degradation sources, see Figure 89.

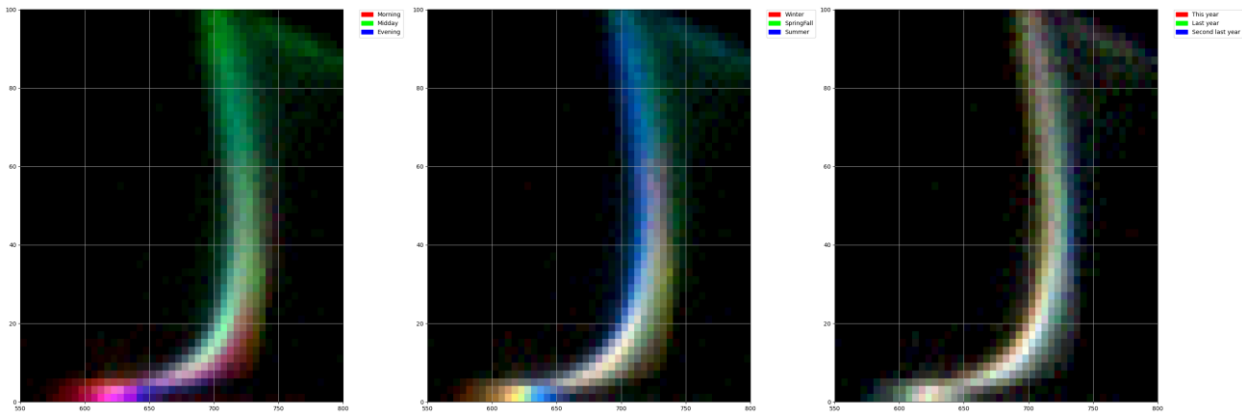


Figure 6: MPP-clouds, displayed as colorized 2D-histograms. In summer (center, blue) the voltage is slightly lower. Also, in the morning hours (left, red) the voltage is slightly larger for low irradiances than in the evening hours. The right graph exhibits that there is no dramatic degradation over time, as red+green+blue are color-mixed to white.

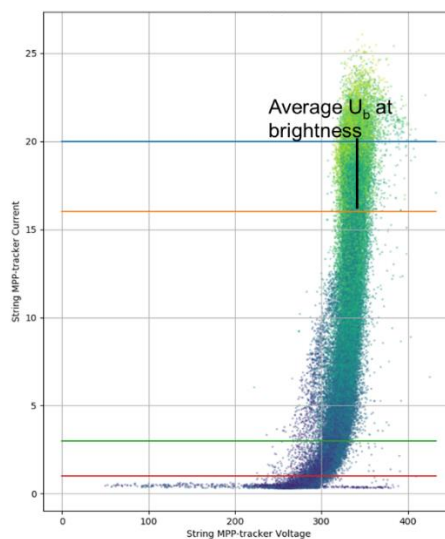


Figure 7: Within the MPP cloud, regions of interest can be defined, e.g. between the orange and blue line. The voltages of the selection band are then analyzed statistically, e.g. the average, standard-deviation, quantiles, or the band structure can be extracted.

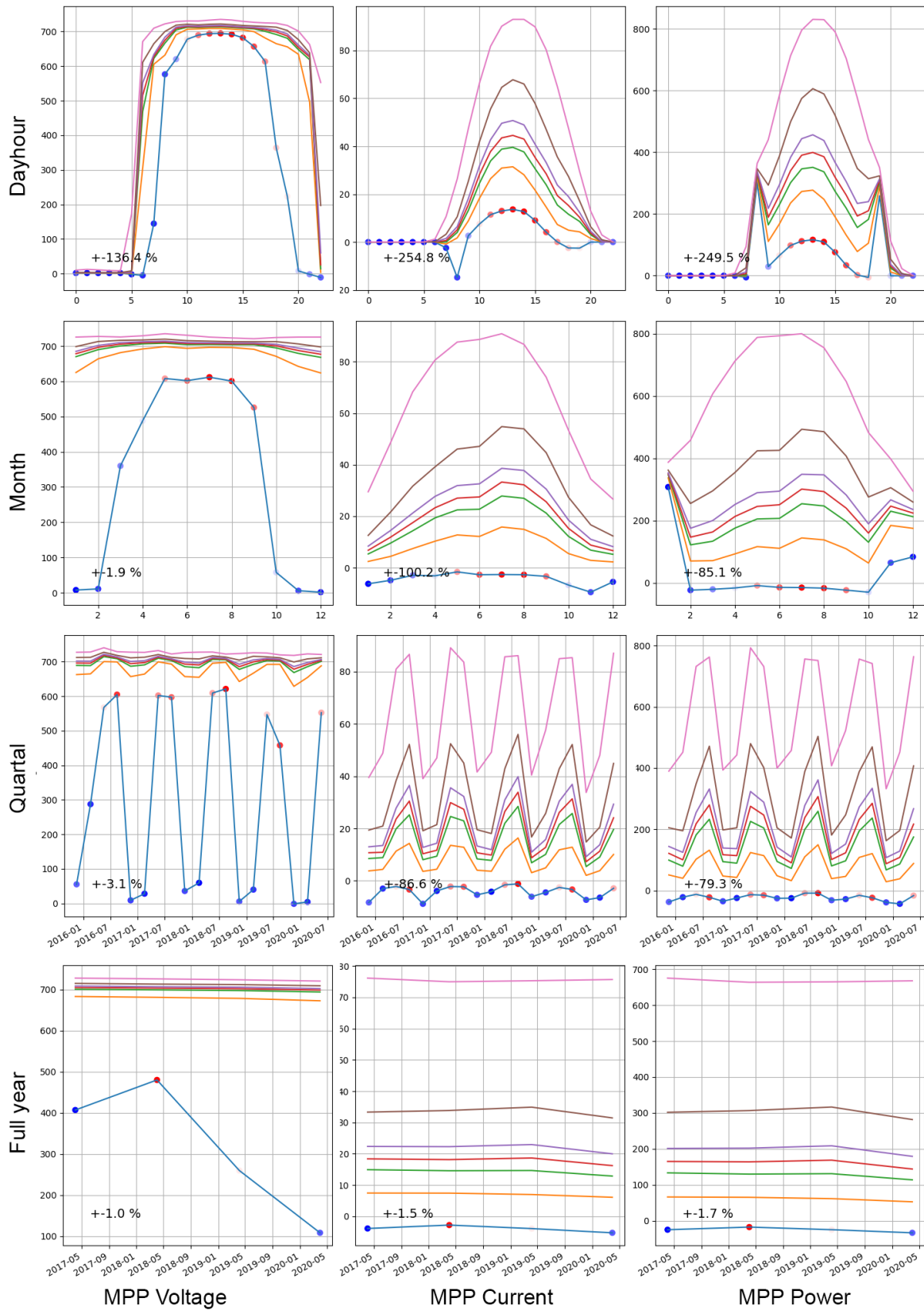


Figure 8: Development of the quantiles extracted from the MPP clouds (10% blue, 33% orange, 45% green, 50% red, 55% violet, 66% brown, 90% pink). This exhibits daily changes, seasonal changes, and long-term changes of relevant metrics.

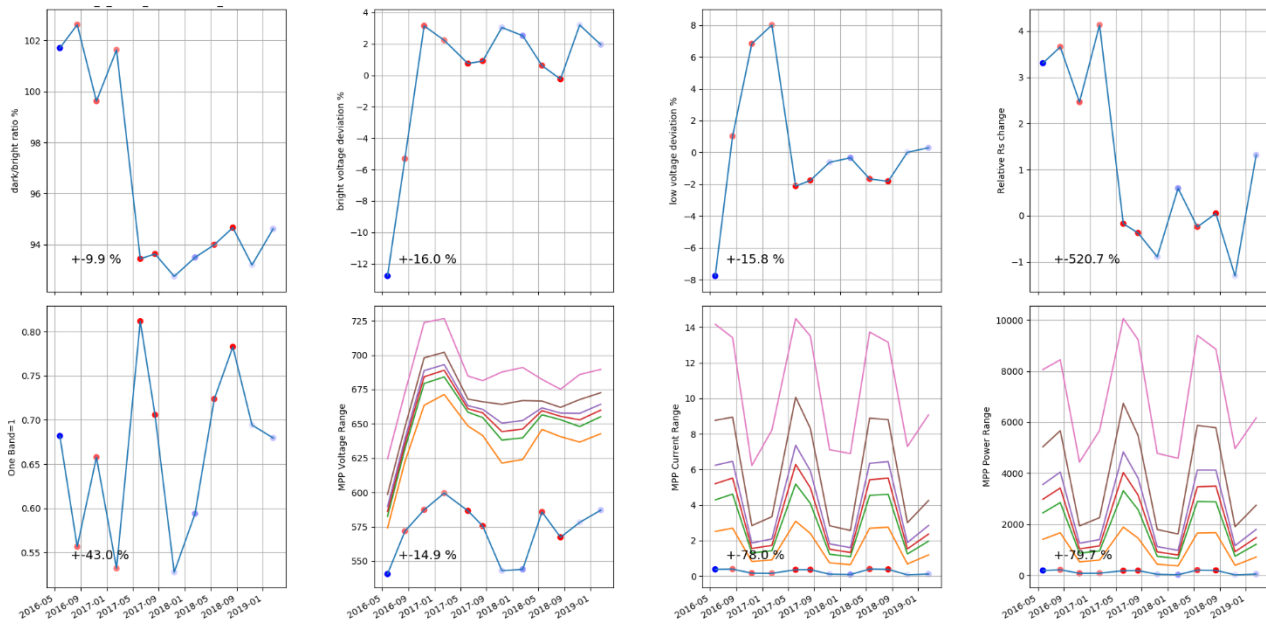


Figure 9: In the full metric graphs, here plotted over the quartals, indicators are given that can be used to indicate potential-induced degradation (PID), shading, serial resistance change, voltage and current degradation.

2. Results of Milestone 2.2

While monitoring larger photovoltaic (PV) generators (“plants”), typically there are three different sources of data: data recorded by inverters, weather sensors, and finally the electric meters. Most commonly, data is uploaded to a web-based data aggregation platform.

From there, data can be downloaded for further analysis in text files larger than one gigabyte.

Typical data from inverters contains on the AC side: power, grid frequency and phase currents. On the module DC side, commonly the working point is recorded (U_{mpp} , I_{mpp}) for possibly multiple MPP trackers per inverter.

In the previous milestone document M2.1, analysis of the inverters efficiency behaviour were presented, as well as the behaviour of the inverters DC side, where the MPP tracking behaviour was analysed in combination with the modules string irradiation dependent MPP position. In the following chapters, we will build upon on this output.

2.1 Digital Twins

To analyze long-term degradation of PV modules, one could compare the production at similar environmental conditions between occasions that are distributed over multiple years. It is common to use clear-sky conditions, as the effects of clouds strongly depend on the clouds location on the sky. The problem with this approach is, that clearsky conditions at similar temperatures are hardly ever met, and hence the statistical relevance is very limited.

To obtain better statistics, one creates a model of the PV production based on measured factors (“observables”, e.g. air or module temperature, irradiation, wind speed) and derived features (solar sky position, clearsky irradiation). The ratio of the actual production to the predicted production then can be evaluated. While this can be done with the most fine grain time resolution, better statistical relevance can be obtained by temporal averaging over longer periods.

There exists the standard „IEC 61724-1“, 14.3.2 „Temperature-corrected performance ratios“, which defines a simple procedure. The digital twin in this case is a simple model: $P = G / 1000 * W_p * [1 + \alpha(T - 25)]$, with the predicted AC Power P, the in-plane irradiation G, the installed Module Peak Power at STC, and the temperature coefficient of the module MPP power (typically $-0.42 * 0.01 / ^\circ$). This is a very simple, linear digital twin of the PV production.

However, it does not include the decrease of PV power under lower loads, a combination of decreased inverter efficiency and the parallel resistance production power drop of the modules themselves. This effect can be included by three more fit variables. Thereby, the overprediction of standardized performance ratio can be decreased, leading decreased seasonality of the PR, see Figure 1.

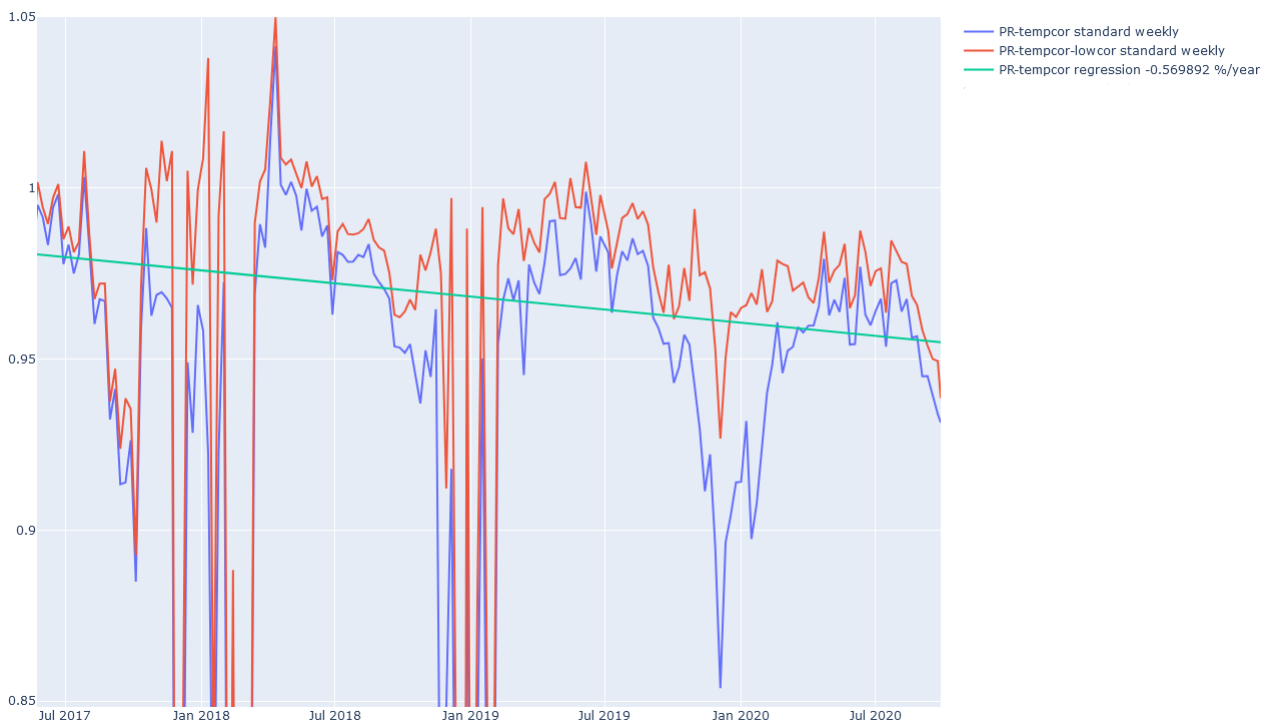


Figure 10: The monthly averaged PR of an Austrian PV-Plant according to standard (blue) and with improved low-light accuracy (red). Deviations occur mainly under snow conditions, if the modules are covered but the irradiation sensor is not. A robust linear fit exhibits the yearly power degradation.

Improved digital twins are necessary to exhibit smaller deviations of the PV production, see Figure 21. They require the tilted plane clearsky irradiation which can be calculated from the GPS location and the time of day using common radiation models such as “Perez”¹. As typically neither the orientation nor the factual installed power is known, they need to be obtained based on monitoring data.

¹ Perez, R. et. al 1988. “The Development and Verification of the Perez Diffuse Radiation Model”. SAND88-7030

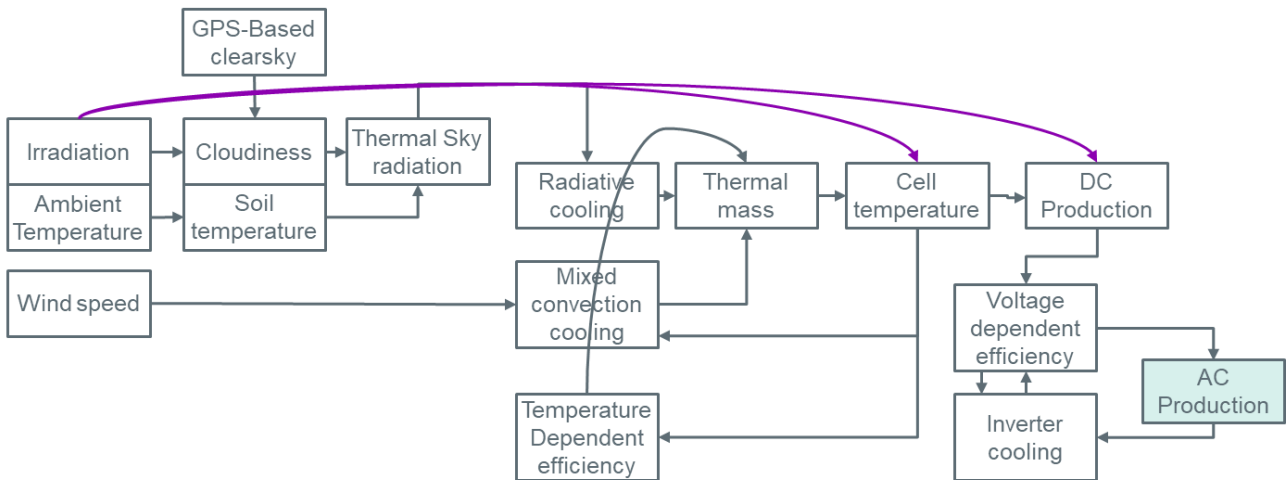


Figure 11: An analytic digital twin of PV production: From irradiation and the calculated tilted clearsky-irradiation the cloudiness can be estimated. This has impact on the infrared radiative balance that affects 50% of the modules cooling. The hysteretic cell temperature then influences the DC production, which by a simple inverter model creates the feed in power.

2.1.1 Timestamp validation and orientation estimation

Inverters typically have a quartz resonator as time source. This quartz is tuned to a specific operating temperature and is known to deviate of up to 30min/year in other climatic zones, if not regularly updated by online time servers. Additionally, problems with time zones and summer/winter time switching are fairly common.

By estimation of sunrise/sunset from the inverters data, and comparison to synthetic GPS-based values, the time system can be validated, and deviations be corrected. This can be done for each individual inverter, as well as the radiation sensors. In an observation interval, the values can be averaged over a period, or sampled at one instance. If this is done differently for the radiation sensor and the production, a timeshift of half the sampling period is observed.

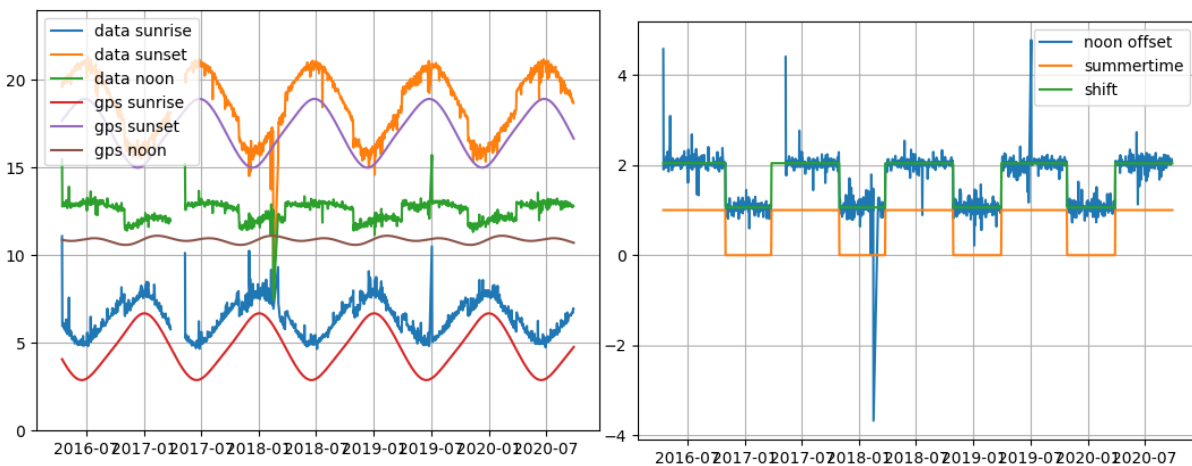


Figure 12: Validation of time stamps. Horizontally the days of multiple years, vertically the dayhour/hour difference.

Once the timezone and summer/wintertime behavior of the monitoring data is established, the orientation of the section of the PV plant can be found by numerical optimization. The comparison of the directional clearsky radiation to the observed peak irradiation, see Figure 13, can be used to create a shadow map in Figure 14:

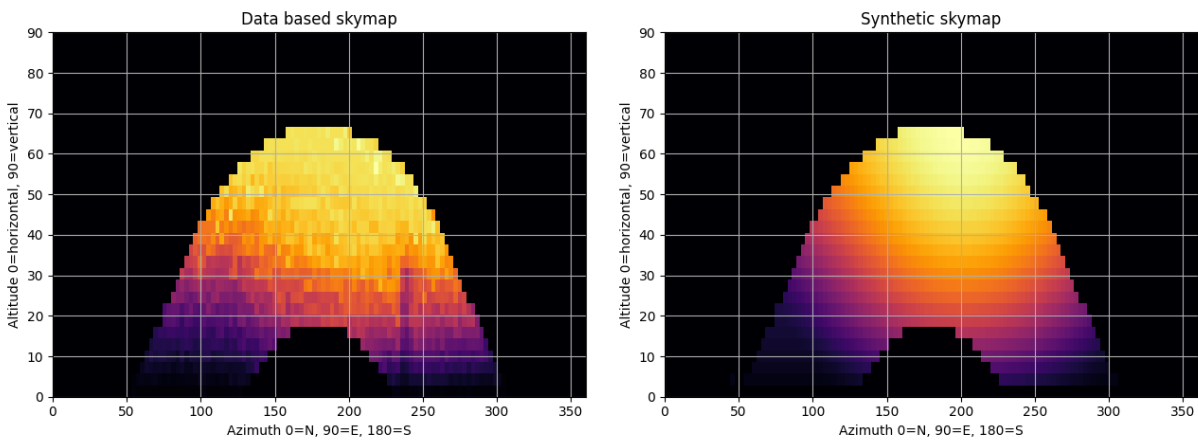


Figure 13: Comparison of data based clearsky irradiation plotted over the hemisphere, to synthetically clearsky irradiation for the fitted optimal orientation.

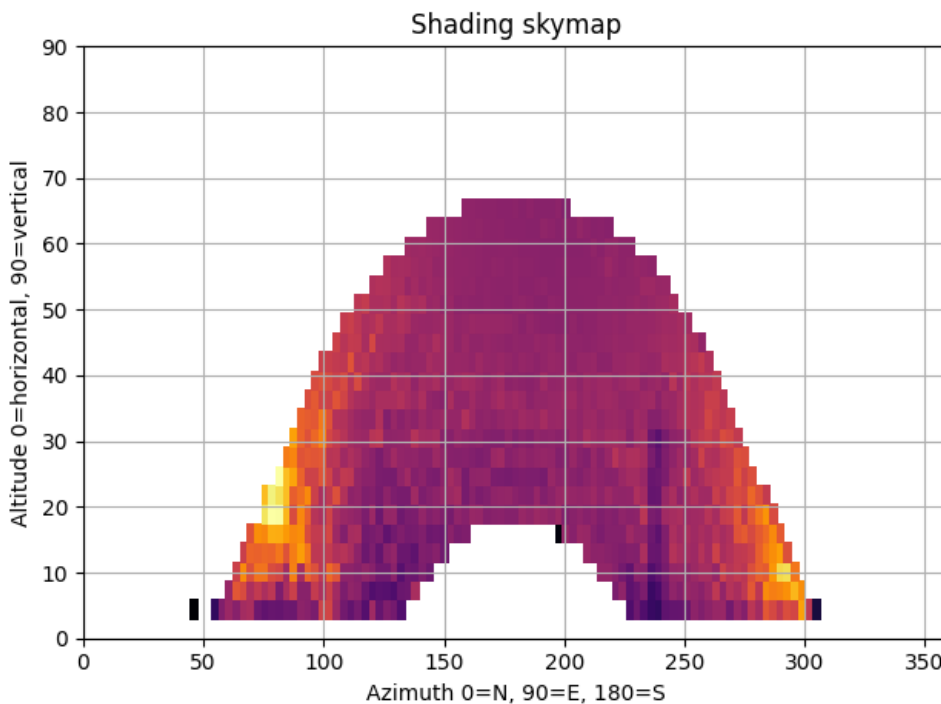


Figure 14: The ratio of the synthetic and databased irradiation skymap shows directional shading, in this case a tower in the west of the system.

As soon the orientation of the plant is known, the tilted clearsky irradiation can be calculated using common radiation models, e.g. “Perez”. As the majority of large PV systems have an irradiation sensor (typical accuracy 5%, typically worse below 200W/m²), the ratio of the measured irradiance and the calculated clearsky irradiance can be estimated. The value named “cloudiness” is typically ranged between 0 and 1.2, where values above 1 are caused by unhindered direct irradiation and bright clouds outside of the suns direct trajectory.

Typical weather forecasts contain a value representing the amount of cloud cover, but as the location of the

clouds matter, there is only a week correlation between the meteorological cloud cover and the cloudiness as defined before.

2.1.2 Data reduction for model fitting

Rapid changing ambient conditions, i.e. a compact cloud moving in front of the sun, can create changes in the modules current-voltage curves, and hence in the MPP point. The inverter sometimes needs some time to regulate to a new ideal setpoint, and while the tracking is performed will create deviations of the production that cannot be explained by a simplified digital twin. Hence, it is useful to decrease the importance of such data points while numerically fitting system parameters of a simple digital twin, see Figure 23. During the fit, one can either give each point a weight/importance that is defined the stability of the conditions, or remove points with insufficient stability altogether.

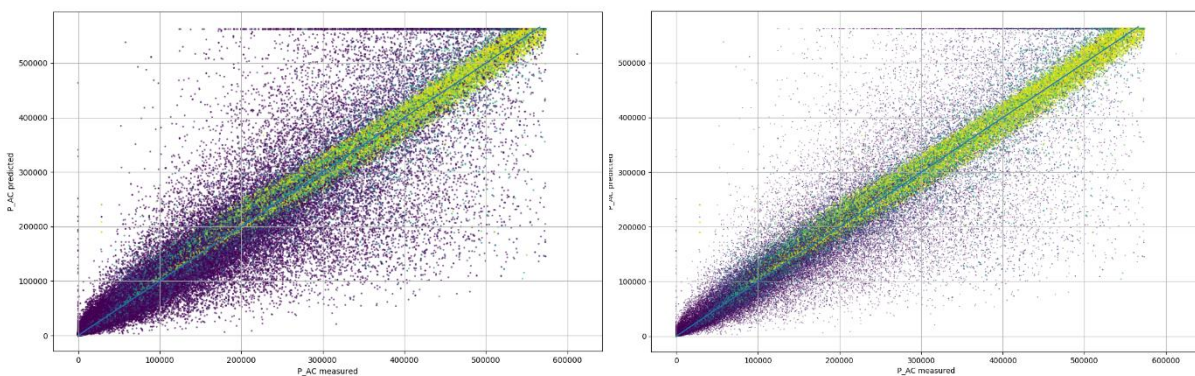


Figure 15: The correlation between the production predicted by a digital twin (vertical) over the measured production (horizontally). Left, the points are drawn with equal weight/dot size. Right: with a decreased point size for instable conditions.

2.1.3 Evaluation of the digital twin

After the fitting, the historical environmental data can be evaluated using the twin, and from the predicted production the observed production can be subtracted. This can be normalized to a peak production, e.g. found by a 99% percentile of the AC production, to obtain relative deviations.

In a next step create bins of ambient conditions (e.g. five ranges of irradiation) are defined and used to create histograms of the relative predictor deviations for each of the bins, see Figure 29. For each bin, the mean (systematic under/overestimation) as well as the standard-deviation (typical prediction error) can be calculated. Furthermore, the binning can not only be done in one dimension but be performed two-dimensionally using both irradiation and ambient temperature. This classified expected error enables not only to predict the production, but also the uncertainty of the digital twin, see Figure 30.

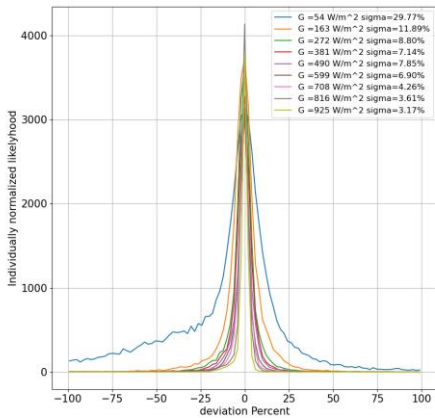


Figure 16: The histograms of relative deviations between digital twin and actual overserved production, depending on a one-dimensional binning of the irradiance. The larger the irradiation, the lower the deviation.

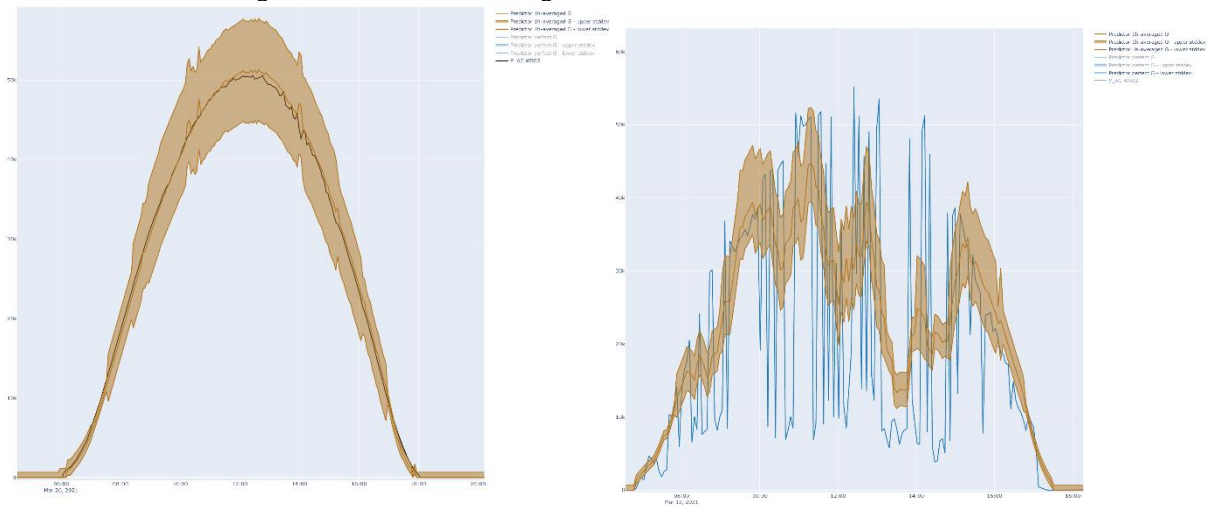


Figure 17: Comparison between measured production (left: black, right: blue) and expected deviations (brown band). Left: on a clear day, right on a day with volatile cloud cover.

2.2 PID

Potential induced degradation is caused by a voltage applied between the frame of the module and the interconnected cells. If the voltage is larger at the frame, it creates an electrostatic field that can cause galvanic drift of Na⁺ ions out of the glass onto the cell surface. There, microscopic spikes might be created that pierce through the PN junction, ultimately causing a short circuit. As the field is stronger close to the edges of the module, initially outer cells are damaged first. Also, this only happens if the cells voltage is more negative than the frame, and increases in intensity with the voltage difference. Hence, most often, only the most negative modules are affected.

Electrically, both a healthy and a short-circuited cell can be described within the framework of the diode model, where the defect is represented by a decreased parallel resistance.

The effect of a varying number of cells damaged by decreased parallel resistance can be simulation, see Figure 18. Thereby it is visible, that PID causes a voltage decrease, initially only at low light settings. With increasing PID, larger and larger currents are affected, until in later stages a general voltage decrease is noticeable.

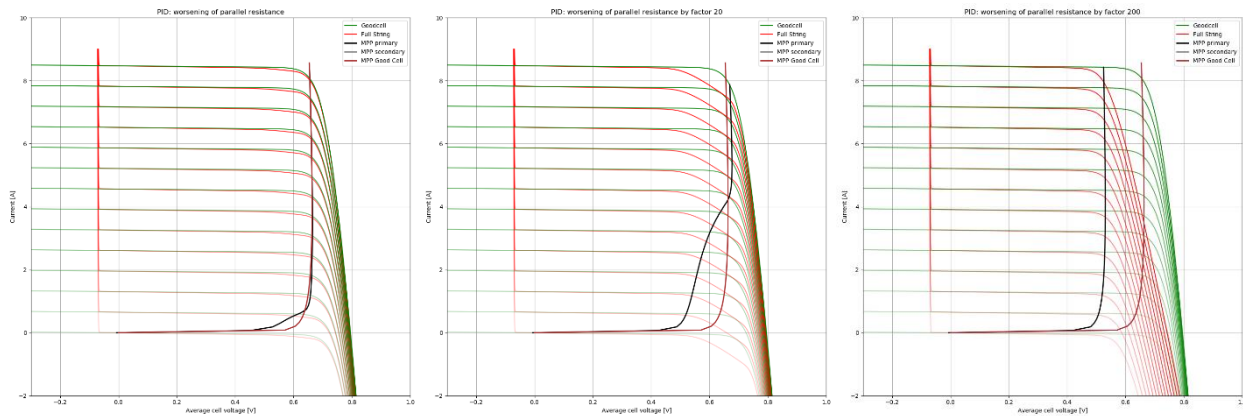


Figure 18: Simulation of the effect of PID on module strings. Bright voltage (horizontal) and current (vertical) characteristics are shown for damaged (red) and undamaged (green) modules, with varying irradiation. The Black curve describes the position of the MPP point of the damaged string, while the brown curve shows the same of the undamaged string.

Similar to the results of Milestone 2.1, the effects can be found in the clouds of MPP-tracking points, based on the DC voltage and current of individual module strings, see Figure 19.

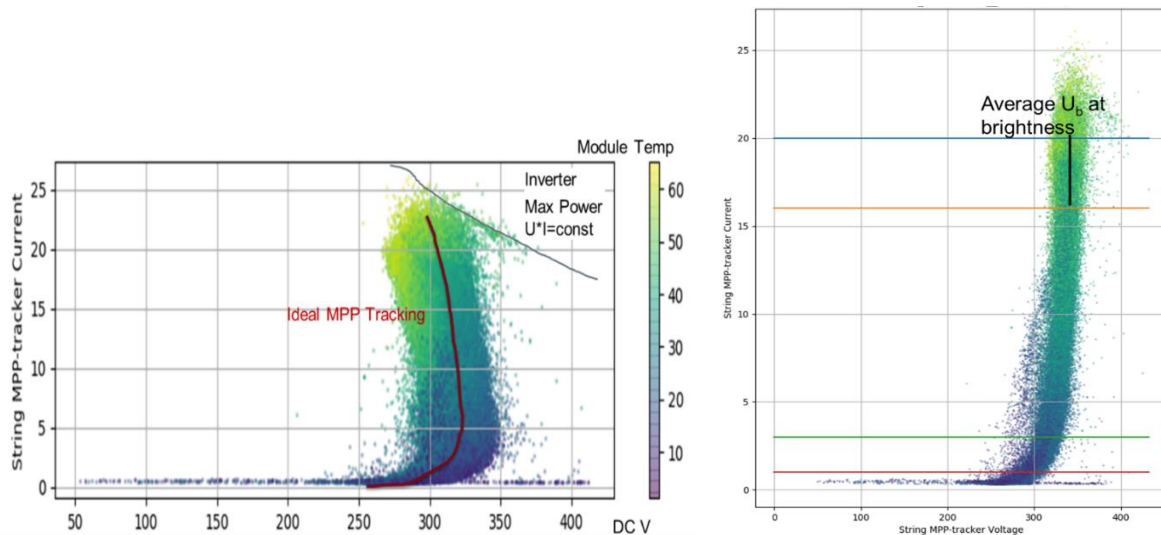


Figure 19: To detect PID, in the MPP clouds (left) described in Milestone 2.1, two current ranges can be defined (right): one at relatively large current (blue-orange) and one at low current/irradiation (red-blue). Within each band, an average voltage can be defined (bright: U_b , dark U_d).

In the onset of PID, a decrease of the ratio U_d/U_b is expected to be observed. For strong PID U_b will decrease over the course of more than six months.

2.3 Soiling

To detect soiling, a naïve approach would be to look at a performance ratio based on a well fitted digital twin. However, in most natural cases the soiling onto the modules will be of similar extend as the soiling onto the irradiation sensor. Hence, it is a good practice to clean such sensors every second week with non-abrasive methods. This is however hardly performed even in multi-gigawatt plants.

There exist dedicated sensors to measure in-field soiling, typically based on the amount of total reflected light within a backlit glass plane. Any dirt would cause external leaking of light and decrease the internal back

reflection. Such sensors are part of the current established standard IEC for monitoring PV systems. However, practical application is lacking, because of the sensors price and the low impact in plant performance.

Purely based on monitoring data, the options to analyze soiling are limited. One approach however is to filter for clearsky day conditions and observe the ratio of the digital twin's production based on the simulated irradiation and the observed production. While this signal will be noisy, the typical 1-6% performance loss might be visible. Typically, one assumes that the soiling absorption is constantly increasing by the so-called soiling rate. During precipitation, the soiling absorption is decreased proportionally to the water amount. These parameters can be fitted to the measured ratios, to obtain a digital twin. As however a strong seasonality is to be expected, e.g. due to pollen, the practical application was found to be limited.

3. Results of Milestone 2.3

In the previous milestone document M2.2, some aspects of the digital Twin were already presented for the use in time series analysis.

Here, we elaborate on further details.

3.1 Digital Twins

To analyze long-term degradation of PV modules, one could compare the production at similar environmental conditions between occasions that are distributed over multiple years. It is common to use clear-sky conditions, as the effects of clouds strongly depend on the clouds location on the sky. The problem with this approach is, that clearsky conditions at similar temperatures are hardly ever met, and hence the statistical relevance is very limited.

To obtain better statistics, one creates a model of the PV production based on measured factors ("observables", e.g. air or module temperature, irradiation, wind speed) and derived features (solar sky position, clearsky irradiation). The ratio of the actual production to the predicted production then can be evaluated. While this can be done with the most fine grain time resolution, better statistical relevance can be obtained by temporal averaging over longer periods.

There exists the standard „IEC 61724-1“, 14.3.2 „Temperature-corrected performance ratios“, which defines a simple procedure. The digital twin in this case is a simple model: $P = G/1000 * W_p * [1 + \alpha(T-25)]$, with the predicted AC Power P, the in-plane irradiation G, the installed Module Peak Power at STC, and the temperature coefficient of the module MPP power (typically $-0.42 * 0.01 / ^\circ$). This is a very simple, linear digital twin of the PV production.

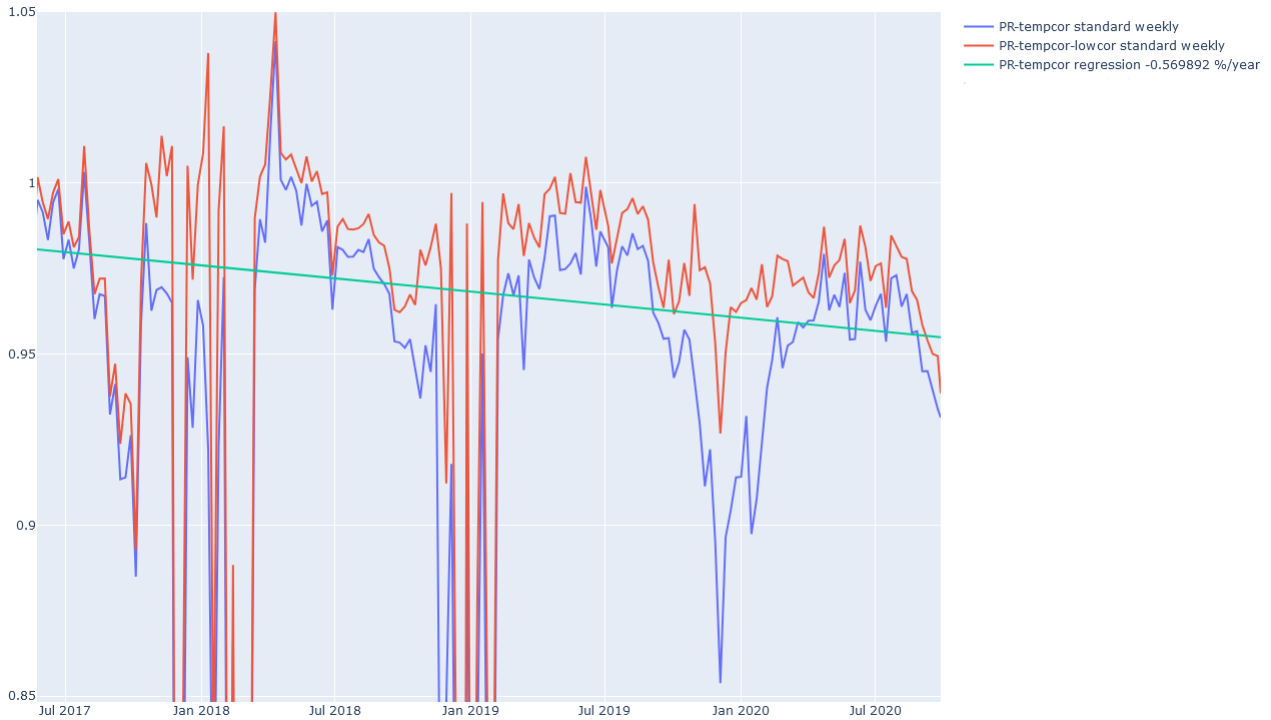


Figure 20: The monthly averaged PR of an Austrian PV-Plant according to standard (blue) and with improved low-light accuracy (red). Deviations occur mainly under snow conditions, if the modules are covered but the irradiation sensor is not. A robust linear fit exhibits the yearly power degradation.

Improved digital twins are necessary to exhibit smaller deviations of the PV production, see Figure 21. They require the tilted plane clearsky irradiation which can be calculated from the GPS location and the time of day using common radiation models such as “Perez”². As typically neither the orientation nor the factual installed power is known, they need to be obtained based on monitoring data.

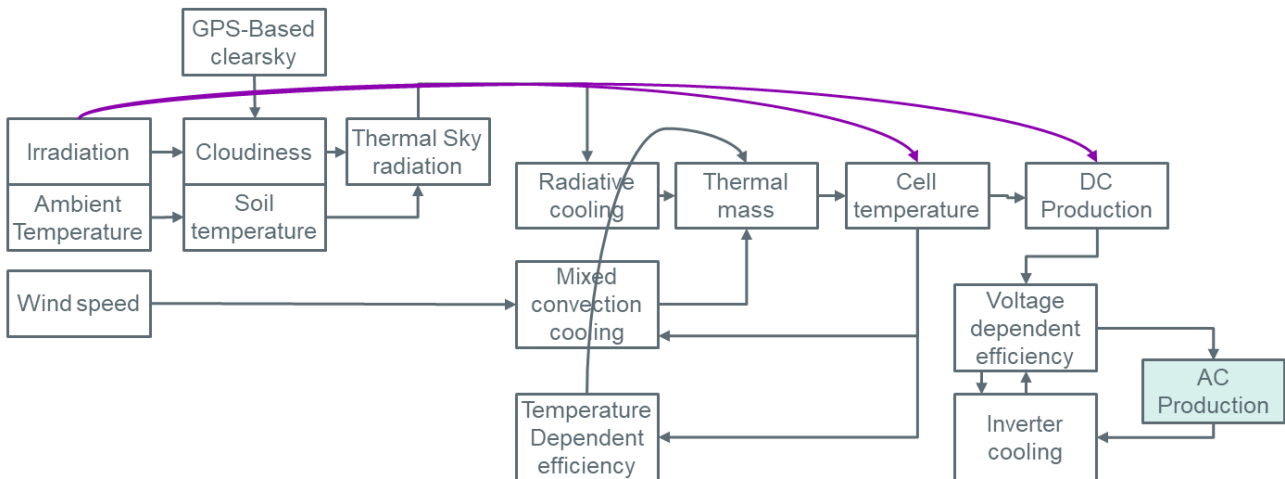


Figure 21: An analytic digital twin of PV production: From irradiation and the calculated tilted clearsky-irradiation the cloudiness can be estimated. This has impact on the infrared radiative balance that affects 50% of the modules cooling.

² Perez, R. et. al 1988. “The Development and Verification of the Perez Diffuse Radiation Model”. SAND88-7030

The hysteretic cell temperature then influences the DC production, which by a simple inverter model creates the feed in power.

3.1.1 Preprocessing

The preprocessing pipeline, see Figure 22, is necessary to obtain the strings direction. This again is a prerequisite to calculate the tilted clear-sky irradiation.

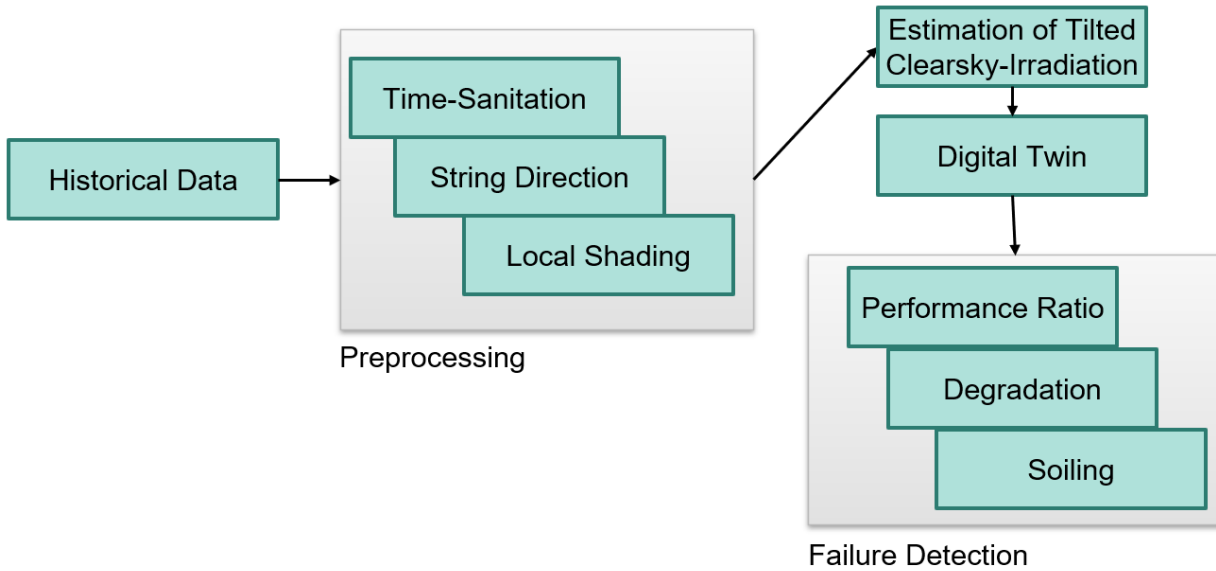


Figure 22: The Pipeline for data pre-processing. The Preprocessing steps were already described in M2.2.

3.1.2 Twin Modeling

Rapid changing ambient conditions, i.e. a compact cloud moving in front of the sun, can create changes in the modules current-voltage curves, and hence in the MPP point. The inverter sometimes needs some time to regulate to a new ideal setpoint, and while the tracking is performed will create deviations of the production that cannot be explained by a simplified digital twin. Hence, it is useful to decrease the importance of such data points while numerically fitting system parameters of a simple digital twin, see Figure 23. During the fit, one can either give each point a weight/importance that is defined the stability of the conditions, or remove points with insufficient stability altogether.

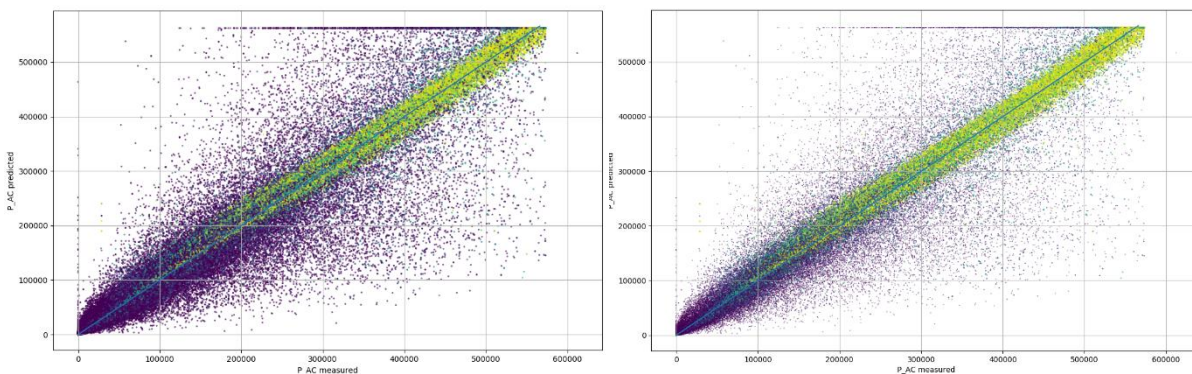


Figure 23: The correlation between the production predicted by a digital twin (vertical) over the measured production (horizontally). Left, the points are drawn with equal weight/dot size. Right: with a decreased point size for instable conditions.

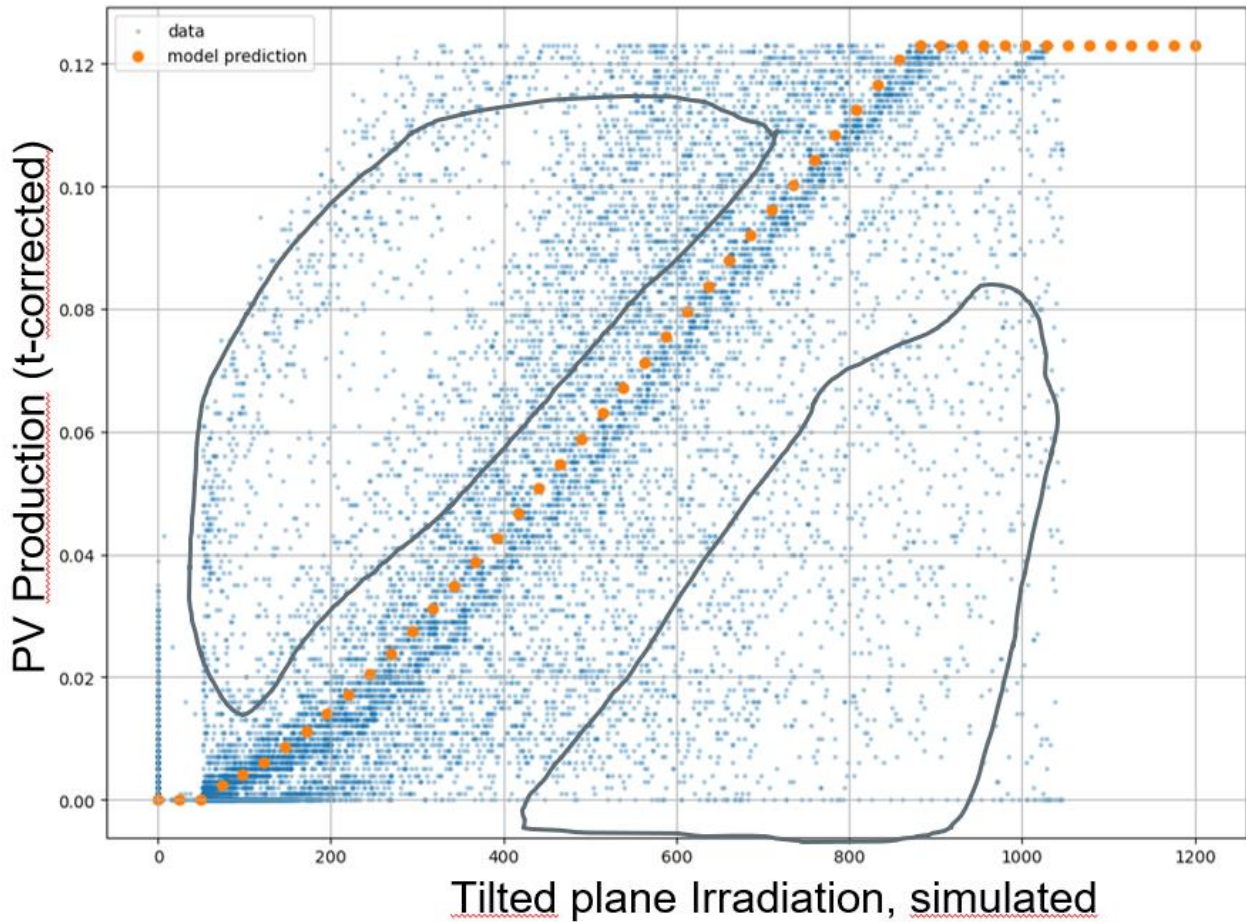


Figure 24: By defining weights to the outliers (clouded conditions and in stationary conditions), the orange curve can be fitted that describes the main information of the digital twin.

Using the simulated tilted clearsky irradiation, that depends on the knowledge of the strings orientation, the graphs in Figure 24 and Figure 25 can be developed. Using numerical optimization, the parameters of the shape of the main curve can be obtained. It is imperative that the used PV production in that case is already temperature compensated.

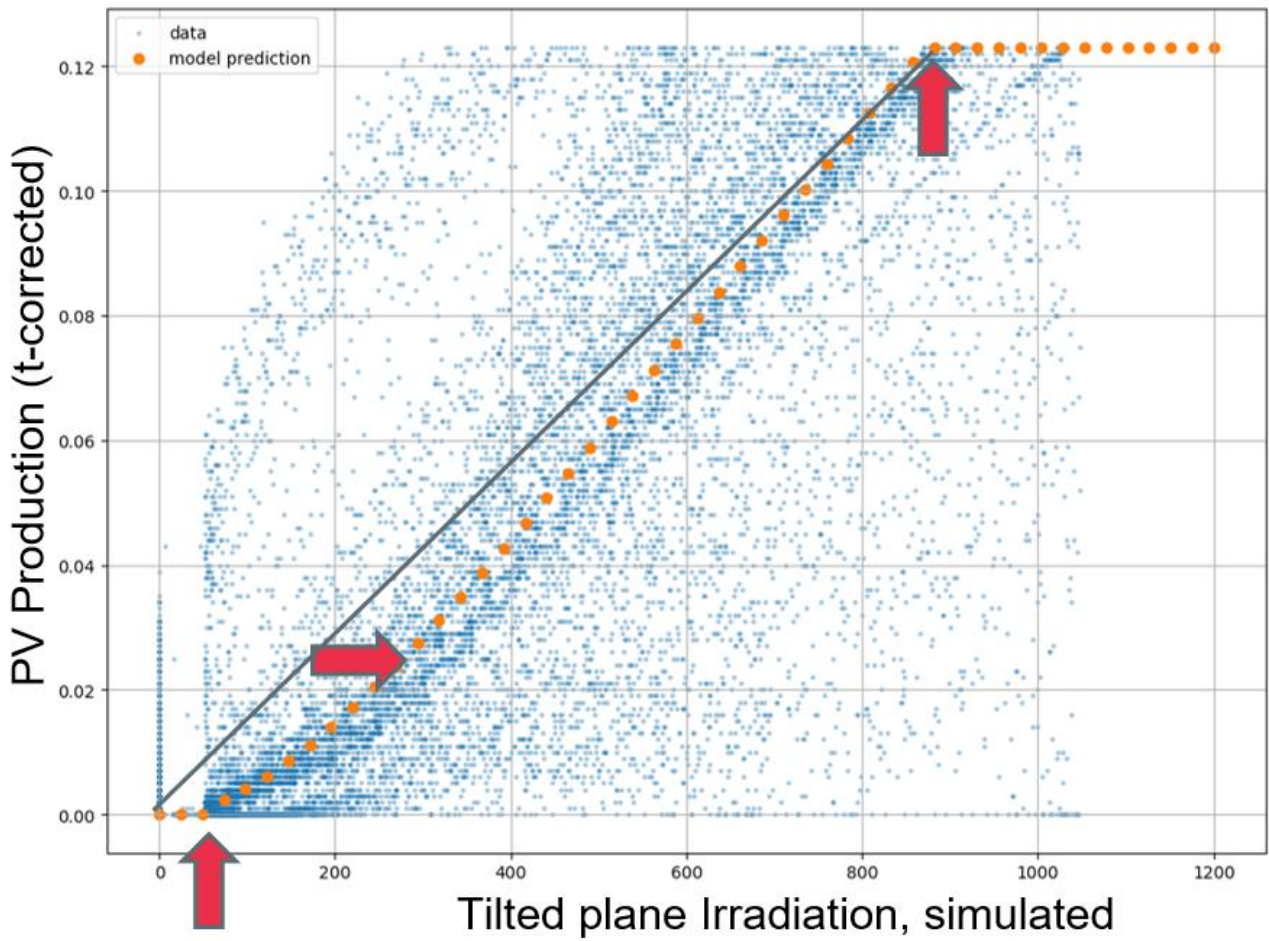


Figure 25: The analytic twin is parameterized by a turn on irradiation, a maximum production, a steepness, and a nonlinear term.

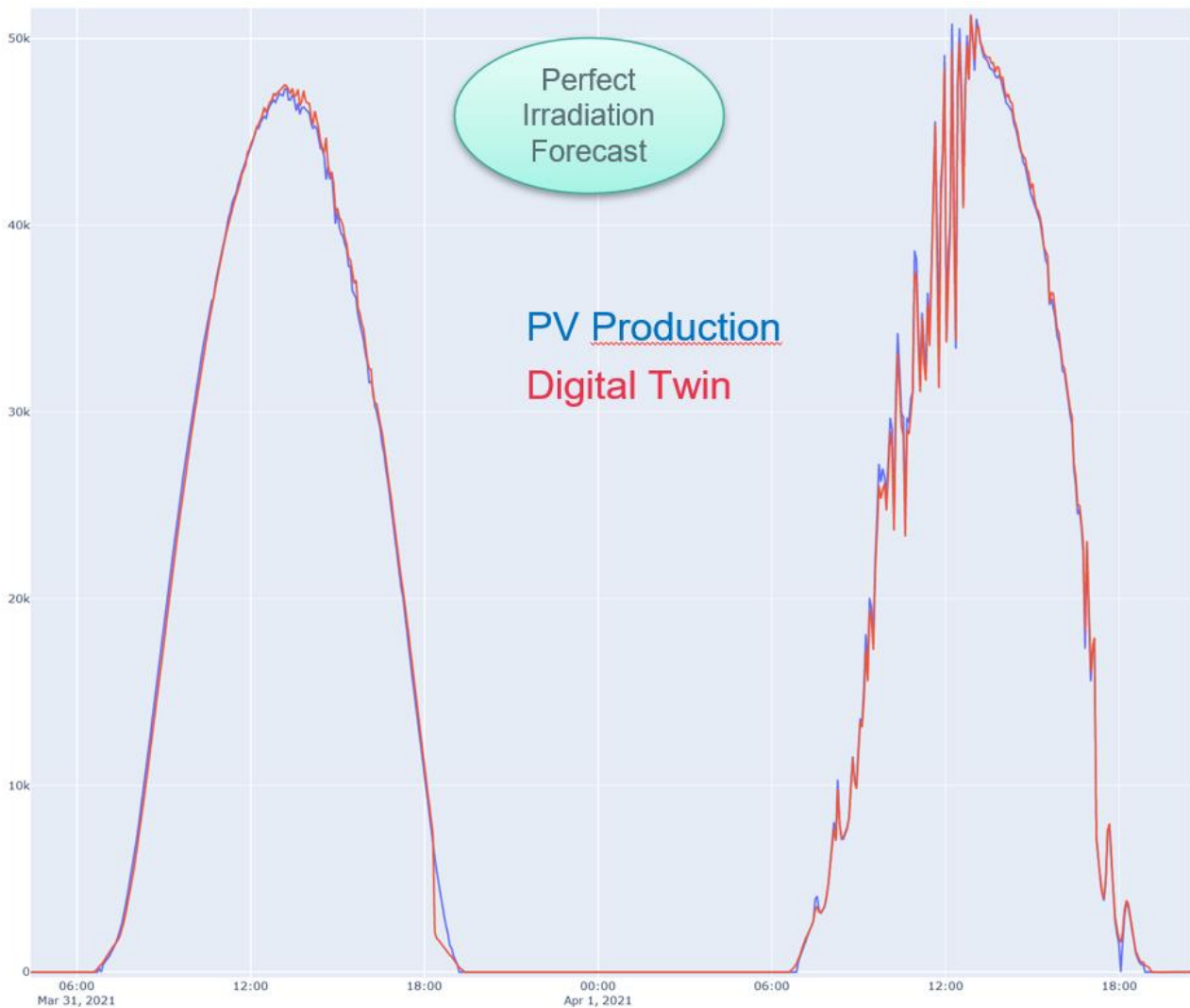


Figure 26: If locally measured irradiation and temperature data is put into the twin, extremely good predictions can be found.

3.1.3 AI assisted twinning

As some predictable aspects of the real world are outside the scope of a simple analytic twin, one can use black box machine learning as an additional step, see Figure 27. This enables to decrease the required intelligence of the machine learning, hence allowing smaller neural networks, less needed training data, and faster learning speed.

Multiple machine learnings were evaluated, and linear regression trees were found most suitable, resulting in an average error of the digital twin of typically 1.2%. Neural networks exhibited a similar accuracy, and multidimensional linear regression did show less accurate results.

This mixed approach, of using a analytic twin together with black box machine learning allows to pick the best parts of both worlds. Intercomparison of plant sections can be performed with the analytic predictor, while unknown predictable effects are modeled by the machine learning.

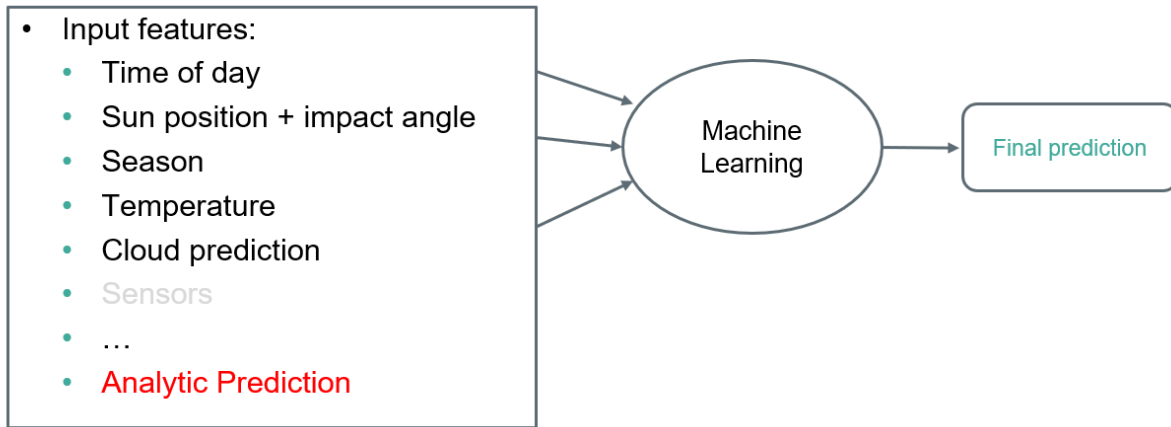


Figure 27: In a further step, the analytic digital twins output is used as an input for generic machine learning.

3.1.4 Prediction of power likelihood

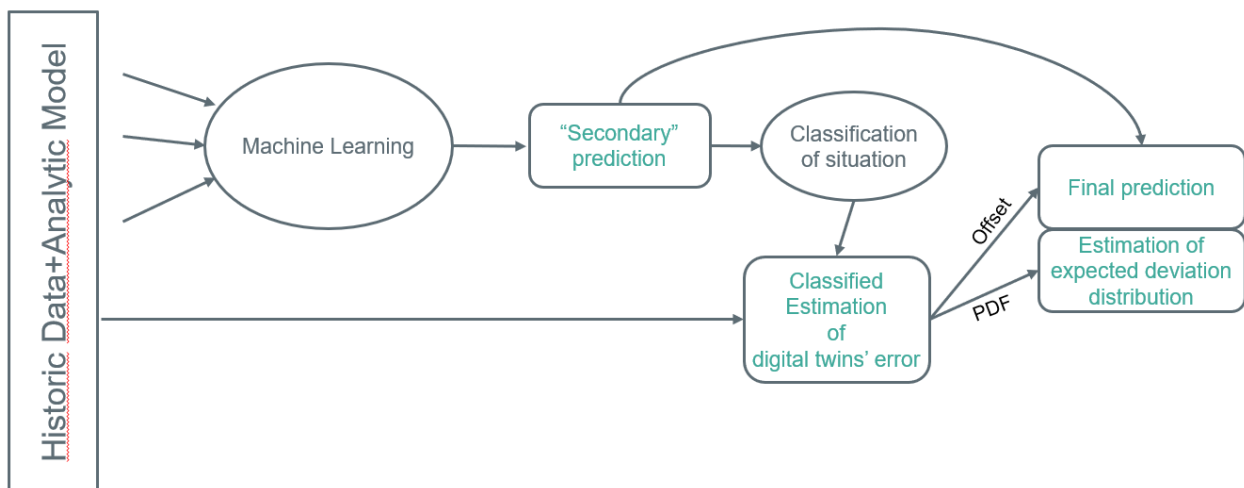


Figure 28: In a further step, the analytic digital twins output is used as an input for generic machine learning.

Different production situations can be grouped to situations, e.g. by grouping the irradiation, and maybe additionally subgrouping the temperature.

Within each group, all observed data values can be compared to the predictor at that time, resulting in a deviation [percent] at that timestamp. All deviations of a “situation” can be grouped, and interpreted as a histogram, see Figure 29.

The histogram represents, a probability density function of the experienced deviations, that can also be used as a predictor for the forecasting inaccuracies.

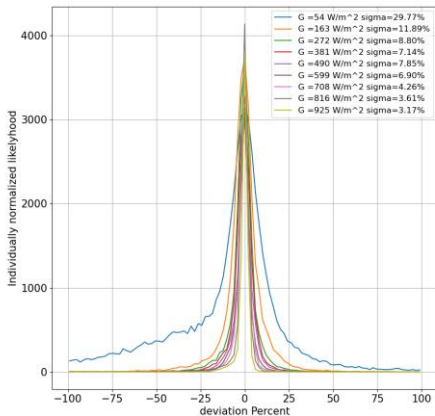


Figure 29: The histograms of relative deviations between digital twin and actual overserved production, depending on a one-dimensional binning of the irradiance. The larger the irradiance, the lower the deviation.

3.1.5 Total prediction digital twin + Uncertainty

In a next step create bins of ambient conditions (e.g. five ranges of irradiation) are defined and used to create histograms of the relative predictor deviations for each of the bins. For each bin, the mean (systematic under/overestimation) as well as the standard-deviation (typical prediction error) can be calculated. Furthermore, the binning can not only be done in one dimension but be performed two-dimensionally using both irradiation and ambient temperature. This classified expected error enable to not only predict the production, but also the uncertainty of the digital twin, see Figure 30.

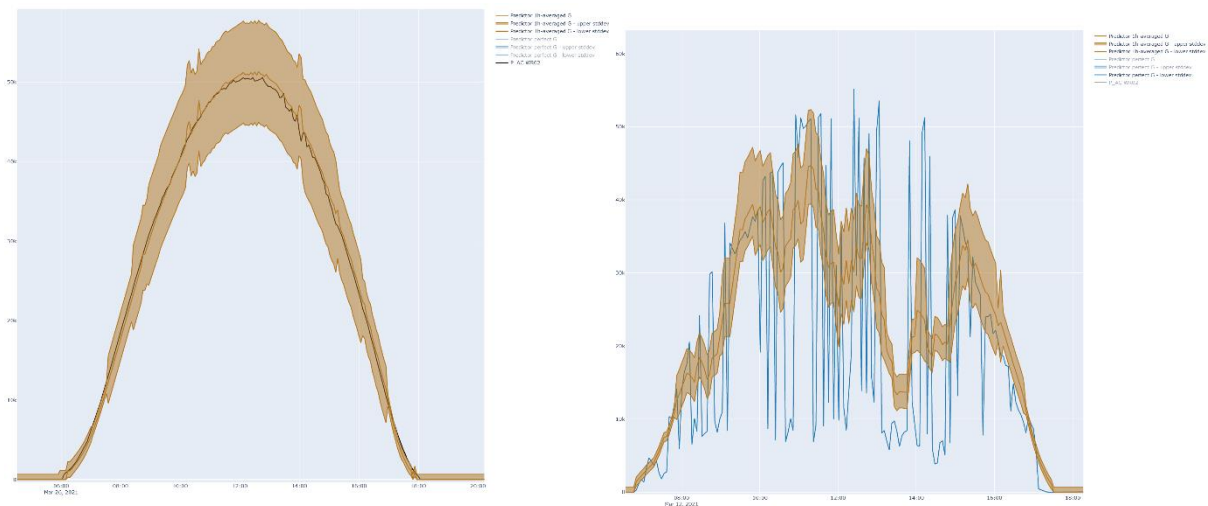


Figure 30: Comparison between measured production (left: black, right: blue) and expected deviations (brown band). Left: on a clear day, right on a day with volatile cloud cover.

3.2 Extrapolation to plants with no history

If the history of a PV plant is not known, also the prediction has limited options. The Analytic digital twin can still be applied, with a few necessary inputs.

- The Peak Power of the plant
- The orientation of the plant
- The turn on-power and max feedin power

The nonlinearity as well as the temperature coefficient can be estimated with other means.

However, the actual power of a section of a PV system typically deviates from the nameplate-values.

Additionally, the assumption of “no plant history” only applies to the first few months of a PV systems lifetime. Thereafter, history data will have an accumulated.

3.3 Revenue Loss

If the digital twin is created for all sections of a PV system, the prediction and the actual feed in can be subtracted. While under normal operating conditions, there should not be a systematic deviation, the time integral of the deviation is close to zero.

However, if the section of the plant is not production, the difference integral will be the predicted production.

Multiplication with the feed in tarif is then able to predict the financial loss.

For this it is however necessary, that the monitoring of the PV system is still active, to record ambient conditions.

If this is not the case, the clearsky irradiation and extrapolated temperature curves can be used.

3.4 System Integration

From most proposed methods in the previous milestones, virtual plots are created that are then used to extract metrics that can be used to trigger errors. These plots can be displayed on demand.

For a learned digital twin, a threshold value for financial loss can be set, so that alerts are triggered if the loss of the settable time alert interval is too large.

How the slow degrading mechanisms should be alerted is still a topic of discussion, as threshold values can only be defined by very experienced personal.